

Multi-order Miniaturized Dual Transmission Zeros HTS Filter without Cross Coupling

Liguo Zhou, Yanshuang Han, Hang Wu, Zhihe Long, Hui Li, and Tianliang Zhang

Abstract—A Miniaturized high temperature superconducting filter applied to mobile communication is designed based on a novel double-folded microstrip hairpin resonator which can be used to adjust the intensity of electromagnetic coupling. The filter has the characteristics of small size and a pair of transmission zeros to improve out-of-band suppression without cross coupling. According to the theory of complex electromagnetic coupling, the circuit structure of the double folded microstrip hairpin resonator is analyzed. By adjusting the lengths of different circuit parts of the microstrip resonator, the exchange of electromagnetic coupling characteristics can be realized, thus introducing transmission zeros. At the same time, the mutual cancellation of electromagnetic coupling can reduce the distance between resonators, so the overall size of the filter is reduced. A double transmission zeros miniaturized microstrip HTS 11-order filter with the center frequency of 1300MHz and bandwidth of 200MHz without cross-coupling is designed. The measured indexes of the filter at 77 K: the center frequency is 1300 MHz, 3 dB relative bandwidth is 15%, in-band insertion loss is less than 0.25 dB, the size is 24.81 mm × 11.60 mm ($0.26\lambda_{gc} \times 0.12\lambda_{gc}$), and out-of-band rejection is more than 70dB. The overall size test results are consistent with the simulation results.

Index Terms—High temperature superconductivity (HTS), filter, transmission zeros, cross coupling.

I. INTRODUCTION

With the development of microelectronic technology, the dimension of active devices in the system is getting smaller and smaller. Therefore, the key to determine the volume of RF transceiver front-end is the passive devices in the system. As the most frequently used passive device, the size of filter is the key factor which has significant influence for the volume of RF transceiver front-end. The performance of the filter also has a great impact on the system performance. Therefore, the research on filters has never gone out of the researchers' vision, and the high performance multi-pass filter is a research hotspot which attracting wide attention of scholars in various countries. The HTS material has extremely high unloaded Q value and ideal microwave characteristics. The microwave filter made of this material has very low insertion loss and in-band attenuation, and has good out-of-band suppression characteristics. Therefore, superconducting microwave devices have important

application prospects in the fields of mobile communication, aerospace, resource exploration, military and national defense, etc. HTSC band-pass filters can be used for frequency pre-selection and band compression in the receiver front-end, which are indispensable key components to suppress noise and improve receiver sensitivity. The current development trend is practicality, miniaturization and commercialization [1]. For HTS filter subsystem, refrigeration system is often used to provide suitable working environment in order to enter practical engineering application field. In order to reduce the refrigeration pressure of the refrigerator, shorten the refrigeration time, improve the refrigeration efficiency, increase the usability, the design of simple and miniaturized high performance filter has become a focus. In general, introducing transmission zeros can improve out-of-band rejection and reduce the size of the RF and microwave filters, for example, references [1]-[12], adopt two pairs of CQ structures to introduce two pairs of transmission zeros, thus the out-of-band rejection characteristics is improved. References [3], [4], [6] adopt CT structure and introduce transmission zeros individually. Alternatively, transmission zeros are introduced by loading a single resonator [9], [13], [14]. By introducing the transmission zeros the same out of band rejection can be achieved with fewer resonators, thereby reducing the dimension of the filter. However, the introduction of cross-coupling will change the intensity of the original coupling, thus complicating the simulation of the filter. Introducing transmission zeros into the loaded resonator will increase the overall size of the filter. References [1], [15]-[17] propose a complex coupling theory, but the resonators designed are relatively simple and the coupling characteristics between the resonators are not changed by adjusting the structure of the resonators.

Smaller coupling spacing is required, when the same coupling amount is achieved, thus realizing the miniaturization of the topology plane of the filter, complex electromagnetic coupling is used to design the filter, by adjusting the size distribution of the resonator circuit, make the electromagnetic coupling between them cancel each other, at the same time, proportion value of the electromagnetic coupling adjusted, thus introducing the transmission zeros without cross coupling, and improving the out-of-band rejection characteristics of the filter.

II. DESIGN OF MICROWAVE DOUBLE-FOLDED HAIRPIN RESONATOR

A. Double-Folded Hairpin Resonator

In microwave integrated circuits, band-pass filters generally adopt parallel coupling structures of microstrip

Manuscript received February 24, 2020; revised April 23, 2020.

Liguo Zhou, Yanshuang Han, Hang Wu, Hui Li and Tianliang Zhang are with the School of Aeronautics and Astronautics, University of Electronic Science and Technology of China, Chengdu 611731, China

Zhihe Long is the Department of Mechanical Engineering, City University of Hong Kong, Tat Chee Avenue, Kowloon, Hong Kong, China (e-mail: zhouliguo0710@163.com).

half-wavelength resonators. In order to effectively reduce the size of the filter, a more compact double-folded microstrip hairpin is used in this paper, as shown in Fig. 1. The line width of the resonator is 0.15mm, and the slit width is 0.1mm, which make the structure more compact.



Fig. 1. Double-folded hairpin resonator.

In the HTSC filter design, considering that the loss of HTSC film is extremely small and the phase constant calculated from the two-fluid model is very close to that calculated from the conventional conductor, So adopt the conventional conductor model to simplify the design, and the material parameters of the substrate selected in this design are: $\epsilon_r = 9.8$, $tg\delta = 10^{-5}$, thickness $h=0.5\text{mm}$; HTSC thin film's surface resistance $R_s \approx 500\mu\text{Ohm}$ at 10GHz [15]. λ is the wavelength of the filter at center frequency in free space. When the ratio of the resonator's linewidth w to the plate's thickness h is less than 2, the effective dielectric constant is determined by formula (1), where ϵ_r is the relative dielectric constant of the substrate.

$$\epsilon_{re} = \frac{\epsilon_r + 1}{2} + \frac{\epsilon_r - 1}{2} \frac{1}{\sqrt{1 + (12h/w)}} \quad (1)$$

The length of the half wavelength resonator $\lambda_g = \lambda_0 / \sqrt{\epsilon_{re}}$. In the double-folded hairpin structure, there is not only energy coupling with adjacent hairpins, but also coupling inside itself, which makes the design complicated. The odd and even mode impedances Z_{0E} and Z_{0O} inside the filter are obtained by combining the assumption of sparse inductance matrix of hairpin structure and the low-pass prototype of the filter, and the micro strip's width w and the gap s between the microstrips of the high-temperature superconducting filter can be obtained by iterative approximation from equation (2)-(3).

$$Z_{0E} = F(s/h, w/h, \epsilon_{re}) \quad (2)$$

$$Z_{0O} = G(s/h, w/h, \epsilon_{re}) \quad (3)$$

The length L of coupling can be calculated by odd and even mode wavelengths λ_{ge} and λ_{go} at the center frequency by equation (4).

$$L = \frac{1}{4} [(1-y)\lambda_{ge} + y\lambda_{go}] - \Delta l \quad (4)$$

where y is a weight factor less than 1. Δl is the strip open-circuit termination effect correction term. The length of the resonator finally obtained is shown in Fig. 1.

B. Calculation of Quality Factor (Q)

For the design of coupling filter, the physical size of resonators and the position of each resonator can be determined by determining the coupling coefficient and external Q_e value between resonators. For microstrip filters, usually there are two coupling modes for tap of microstrip filter: direct coupling and indirect coupling, as shown in Fig. 2 below. Generally, there is no essential difference between the two types of taps. Both types of taps are designed to achieve the quality factor Q_e required by the filter. In this paper, the direct tap is analyzed as follows. For the indirect coupling tap, the analysis is the same. When the phase is $\pm 90^\circ$, the change value of angular frequency is:

$$2Q_e \frac{\Delta\omega_{\pm 90^\circ}}{\omega_0} = \pm 1 \quad (5)$$

The on-load quality factor is obtained by transformation:

$$Q_e = \frac{\omega_0}{\Delta\omega_{\pm 90^\circ}} \quad (6)$$

When h_1 and h_2 take different values in Fig. 2(a), the value of quality factor Q_e obtained according to formula (6) is as shown in Fig. 3 below. For different h_1 and h_2 , the external quality factor tends to decrease first and then increase, and the range is wide. Then, according to the design requirements of the filter, the required Q_e value can be obtained by searching the curve in the figure. In addition, experience shows that in generally, the closer the tap is to the middle of the half-wavelength microstrip line, the larger the quality factor is, and the more suitable it is for the narrow-band filter.

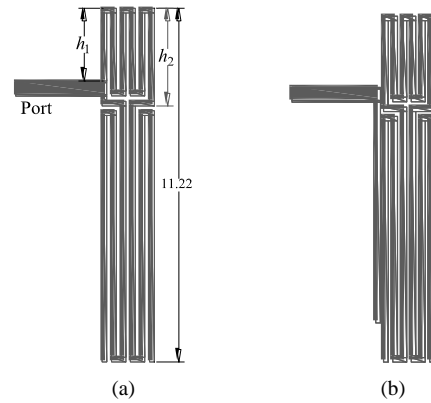


Fig. 2. Resonators with different type: (a) Direct coupling, (b) Indirect coupling.

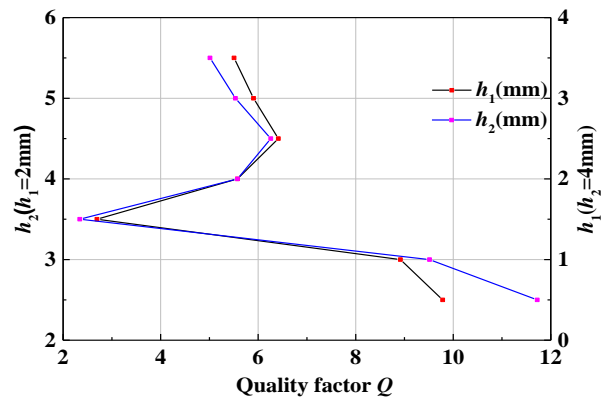


Fig. 3. Curve chart of quality factor when h_1 and h_2 take different values.

III. ANALYSIS OF ELECTRICAL AND MAGNETIC COUPLING CHARACTERISTICS

A. Hybrid Electromagnetic Coupling

Coupling between resonators refers to the exchange of electromagnetic energy between resonators. Coupling between resonators includes electrical coupling, magnetic coupling and hybrid coupling. Hybrid coupling refers to the simultaneous electrical and magnetic coupling between resonators. Electric energy coupling is far more than magnetic energy coupling, which is called electric coupling. On the contrary, it is called magnetic coupling. In energy exchange, whether the coupling of electric energy or magnetic energy mostly depends on the physical parameters of the coupling structure and the mode distribution of electromagnetic field in the resonator, which provides design guidance for the acquisition of electromagnetic coupling characteristics. In general, electromagnetic hybrid coupling is the main form of coupling in planar microstrip circuits.

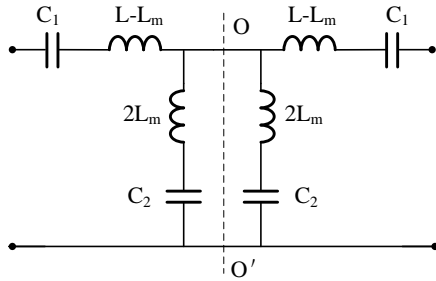


Fig. 4. Equivalent circuit of hybrid electromagnetic coupling.

Fig. 4 is an equivalent circuit diagram of hybrid electromagnetic coupling, where in:

$$C_1 = \frac{C \cdot C_m}{C_m - C} \quad (7)$$

$$C_2 = \frac{C_m}{2} \quad (8)$$

The inductance and capacitance of odd mode and even mode can be obtained as follows:

$$L_{odd} = L - L_m \quad (9)$$

$$C_{odd} = \frac{C \cdot C_m}{C_m - C} \quad (10)$$

$$L_{even} = L + L_m \quad (11)$$

$$C_{even} = \frac{C \cdot C_m}{C_m - C} \quad (12)$$

Thus, odd-mode and even-mode resonant frequencies based on odd-even mode inductance and capacitance are respectively expressed as follows:

$$\omega_{odd} = \sqrt{\frac{1}{L_{odd} \cdot C_{odd}}} = \sqrt{\frac{C_m - C}{(L - L_m) \cdot C \cdot C_m}} \quad (13)$$

$$\omega_{even} = \sqrt{\frac{1}{L_{even} \cdot C_{even}}} = \sqrt{\frac{C_m + C}{(L + L_m) \cdot C \cdot C_m}} \quad (14)$$

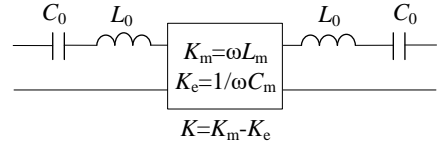


Fig. 5. Equivalent circuit diagram of hybrid electromagnetic coupling.

Suppose E_c is the electrical coupling coefficient and M_c is the magnetic coupling coefficient, as shown in Fig. 5. The coupling coefficient K is:

$$K = \frac{K_m - K_e}{\omega_0 L} = \frac{\omega_0 L_m - 1/\omega_0 C_m}{\omega_0 L} = \frac{L_m}{L_0} - \frac{C_0}{C_m} \quad (15)$$

$$\frac{L_m}{L_0} - \frac{C_0}{C_m} = M_c - E_c = \frac{\omega_{od}^2 + \omega_{ev}^2}{\omega_{od}^2 - \omega_{ev}^2} \quad (16)$$

From equations (13)-(16), the magnetic coupling coefficient and the electrical coupling coefficient can be deduced as follows:

$$M_c = \frac{\omega_m^2 (\omega_{ev}^2 - \omega_{od}^2)}{2\omega_{ev}^2 \omega_{od}^2 - \omega_m^2 (\omega_{ev}^2 + \omega_{od}^2)} \quad (17)$$

$$E_c = \frac{\omega_{ev}^2 - \omega_{od}^2}{\omega_{ev}^2 + \omega_{od}^2 - 2\omega_m^2} \quad (18)$$

According to the definition of electromagnetic coupling coefficient, the following result is obtained:

$$\frac{M_c}{E_c} = \frac{L/L_m}{C_m/C} = \frac{LC}{L_m C_m} = \frac{\omega_m^2}{\omega_0^2} \quad (19)$$

From Equation (18), it can be obtained that the positions of the transmission zeros depend on the ratio of the magnetic coupling coefficient to the electrical coupling coefficient in the circuit. When the intensity of magnetic coupling and electrical coupling are closer, the transmission zero f_m is closer to the center frequency f_0 , which provides a theoretical guidance for adjusting the transmission zeros by adjusting the intensity of electromagnetic coupling.

B. Calculation of Coupling Coefficient

The coupling between resonators mentioned above can be divided into electrical coupling, magnetic coupling and hybrid coupling. In addition, for different coupling structures, the resonators have different self-coupling, and their forms are different from the inter-stage coupling, but all satisfy coupling formula (20), which represents the ratio of coupling energy to stored energy.

$$k = \frac{\iiint \varepsilon E_1 \cdot E_2 dv}{\sqrt{\iiint \varepsilon |E_1|^2 dv + \iiint \varepsilon |E_2|^2 dv}} + \frac{\iiint \mu H_1 \cdot H_2 dv}{\sqrt{\iiint \mu |H_1|^2 dv + \iiint \mu |H_2|^2 dv}} \quad (20)$$

where, μ , ε , E , H , K respectively represent permeability, electrical constant, electric field vector, magnetic field vector and coupling coefficient. In the formula, on the right side is the superposition of electric coupling and magnetic coupling. Coupling coefficient can be positive or negative. When the coupling coefficient is positive, the stored energy

of the resonator will increase. On the contrary when the coupling coefficient is negative, the stored energy of the resonator will decrease. For coupling filters, the self-resonance frequency of resonators may be the same or different.

When the self-resonance frequency of the resonators are different, the calculation formula of the coupling coefficient of each resonators can be obtained:

$$k = \pm \frac{1}{2} \left(\frac{f_{02} + f_{01}}{f_{01} + f_{02}} \right) \sqrt{\left(\frac{f_{p2}^2 - f_{p1}^2}{f_{p2}^2 + f_{p1}^2} \right)^2 - \left(\frac{f_{02} - f_{01}}{f_{02} + f_{01}} \right)^2} \quad (2)$$

When the self-resonance frequency of the resonators are the same, $f_{01}=f_{02}$, the coupling coefficient calculation formula can be simplified as:

$$k = \pm \frac{f_{p2}^2 - f_{p1}^2}{f_{p2}^2 + f_{p1}^2} \quad (22)$$

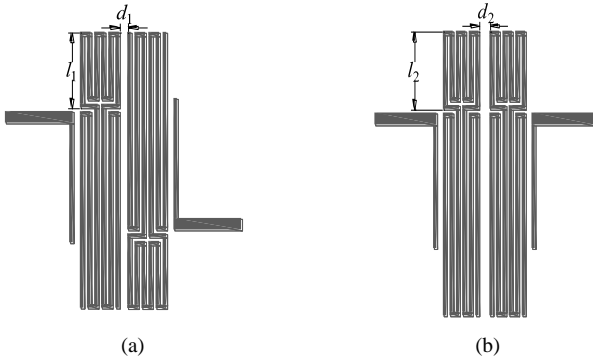


Fig. 6. Different coupling between two resonators (a) Type I, (b) Type II.

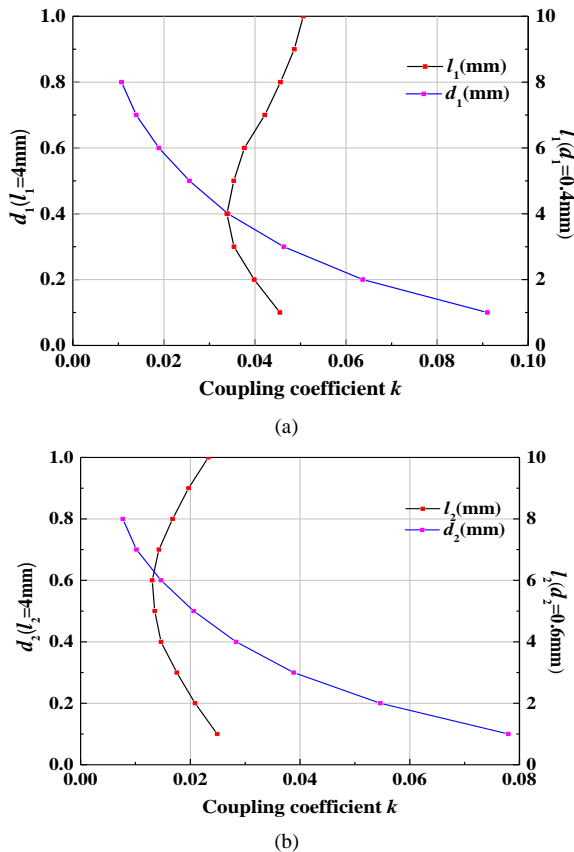


Fig. 7. Relationship between coupling coefficient and resonator size (a) Type I, (b) Type II.

Using the resonator shown in Fig. 1, combined with the indirect tap mode of external coupling, there are two coupling forms between the two resonators as shown in Fig. 6 below. In the case of weak external coupling, the coupling coefficient of different sizes is obtained according to equation (22), as shown in Fig. 7 below.

According to Fig. 7, for the coupling form of type I, when $l_1=4\text{mm}$, the coupling coefficient between the two resonators gradually decreases with the increase of d_1 . When $d_1=0.4\text{mm}$, the coupling coefficient between the two resonators first decreases and then increases with the increase of l_1 . Then there will be a value $l_{1\min}$ of l_1 , which makes the coupling coefficient very small when d_1 is a fixed value. Similarly, for the coupling form of type II, there will be a value $l_{2\min}$ of l_2 . When d_2 is a fixed value, the coupling coefficient will be very small.

IV. DESIGN OF HTS FILTER

A. 4-order Miniaturized Dual Transmission Zeros Filter

The tap adopts the indirect coupling mode mentioned above, and the coupling mode between the two resonators adopts the type II in Fig. 6(b), to design and simulate a 4-order narrowband filter with a central frequency of 1395MHz and a bandwidth of 10MHz. According to Fig. 7(b), there is a value $l_{2\min}$ of l_2 , which makes the coupling coefficient very small when d_2 is a fixed value. If $l_2=l_{2\min}$ is adopted to obtain the same coupling coefficient, the coupling distance between the two resonators will be very small (d_2 is very small), thus reducing the size of the overall circuit. Using a line width of 0.15mm and a slit width of 0.1mm, after simulation and optimization, the circuit structure and size of the finally obtained 4-order microstrip miniaturized filter are shown in Fig. 8 below.

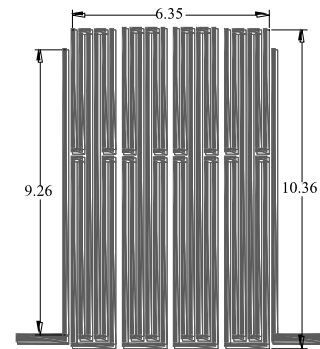


Fig. 8. Planar structure of 4-order miniaturized filter

According to the above analysis of electromagnetic coupling, when l_2 and d_2 are adjusted, the ratio of electric coupling coefficient and magnetic coupling coefficient to electromagnetic coupling will change. Then by adjusting the size of the electrical coupling and the magnetic coupling, on the one hand, the coupling coefficient value described in equation (14) can be adjusted, thus the coupling coefficient between resonators can be adjusted, and then adjusting the overall size of the filter; On the other hand, the ratio of the electromagnetic coupling coefficient can be adjusted. From equation (18), it is known that the positions of the transmission zeros depend on the ratio of the magnetic

coupling coefficient to the electrical coupling coefficient in the circuit, so the change of the transmission zeros can be adjusted simultaneously. By adjusting l_2 and d_2 , the frequency response curves are finally obtained, as shown in Fig. 9 below. There is a transmission zero at 1364MHz and 1399MHz respectively, and the out-of-band rejection characteristic is better than that of the filter without transmission zeros.

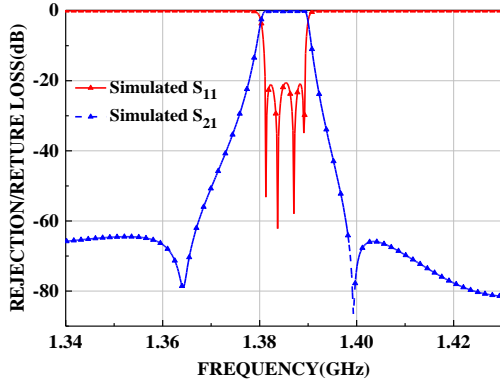


Fig. 9. Simulation of 4-order miniaturized filter.

B. 11-Order Miniaturized Dual Transmission Zeros Filter

According to the generalized Chebyshev prototype design method mentioned in document [8], the filter coupling matrix with symmetrical structure of 11th order, center frequency of 1300MHz, bandwidth of 200MHz and in-band ripple of 0.05dB is obtained as shown in Table I.

TABLE I: THE COUPLING COEFFICIENTS OF THE 11-ORDER HTS FILTER

$M_{1,2}=M_{10,11}$	$M_{2,3}=M_{9,10}$	$M_{3,4}=M_{8,9}$
0.1251	0.0897	0.0836
$M_{4,5}=M_{6,7}$	$M_{5,6}$	
0.0816	0.0809	

Using the direct coupling tap method and the Type I coupling method, an 11-order miniaturized filter is designed on YBCO/MgO/YBCO high temperature superconducting plate with a dielectric constant of 9.8, $tg\delta=10^{-5}$ and a thickness of $h=0.5\text{mm}$. Through simulation and optimization, the planar structure finally obtained is shown in Fig. 10 below. The distance d between resonators is approximately equal to 0.1mm, thus effectively reducing the size of the filter. The overall size of the filter is 24.81 mm \times 11.60 mm ($0.26\lambda_{gc}$, $0.12\lambda_{gc}$). In addition, according to the above analysis, by adjusting l_1 and d_1 of resonators in type I, a pair of transmission zeros can be introduced while minimizing the filter size.

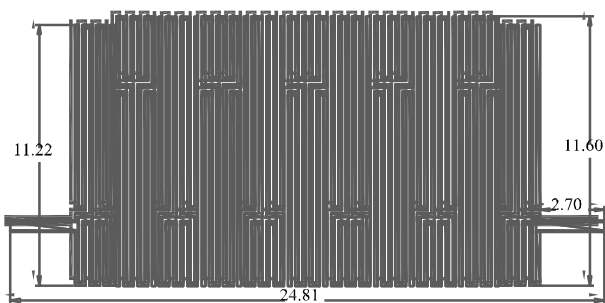


Fig. 10. Plan view of 11-order HTS miniaturized filter.

The electromagnetic simulation software is used for modeling simulation and parameter index optimization, and the S parameter characteristic curve is shown in Fig. 12(a). There are two transmission zeros at the edge of the pass band, which improve the out-of-band rejection of the filter, and the sideband rejection can reach 80dB. The group delay characteristic simulation curve is shown in Fig. 12(b).

Through mechanical processing and photolithography, the physical object of the 11-order HTS filter obtained after assembly is shown in Fig. 11 below.

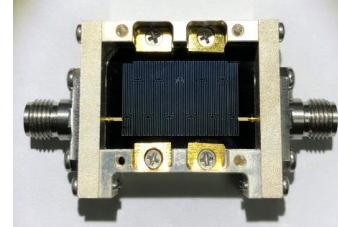


Fig. 11. The physical object of 11-order HTS miniaturized filter.

After the filter is assembled, a performance test is carried out in a low-temperature vacuum test system. When the working temperature is 70 K, the test results of the filter are shown in Fig. 12, wherein Fig. 12(a) shows the comparison between the transmission and reflection characteristics of the filter S parameters and the simulation results, and Fig. 12(b) shows the comparison between the test results of the filter group delay parameters and the simulation results. The specific performance is as follows: the operating frequency of the filter is about 1300 MHz, the relative bandwidth is 15.3%, With the loss of two same connectors, the total insertion loss is less than that of 0.25db, and the return loss is better than 20 dB, the sideband suppression is greater than 80 dB, the group delay in 70% passband is less than 5ns, the input and output impedances of the filter are 50 Ω . The test results of the filter are consistent with the simulation results, thus our idea is verified.

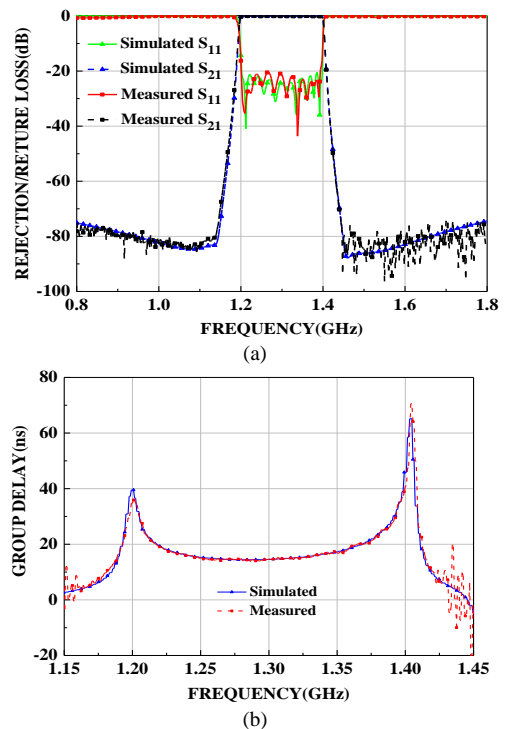


Fig. 12. Simulation and test curves of 11-order HTS miniaturized filter:(a) S parameters,(b) Group delay.

V. CONCLUSION

Based on the resonator that adjusts the strength and characteristics of electromagnetic coupling by changing the proportional distribution, a design method of miniaturized planar filter without cross-coupling is proposed, which is based on an analysis of electromagnetic coupling to introduce a pair of transmission zeros. Based on this theoretical analysis, a 4-order HTS filter with the relative bandwidth is 0.7% and a broadband filter with the relative bandwidth is 15.3% have been designed successfully, both of which have a pair of transmission zeros. The equivalent circuit, theoretical curve, coupling matrix, design process and simulation results of the filter are given, proved the consistency of theoretical analysis and simulation. Finally, the filter with a center frequency of 1300 MHz and the relative bandwidth of 15.3% is designed on the high-temperature superconducting thin film. The superconducting filter with excellent technical indexes is realized. The filter structure design is the premise, the uniform superconducting thin film material is the foundation, and the fine microstrip circuit processing is the guarantee. The test results of the filter is in good agreement with the simulation, and the satisfactory experimental results are obtained. The design and manufacture of the multi-order cross-coupling miniaturized dual transmission zeros superconducting filter are successfully realized.

CONFLICT OF INTEREST

The authors declare no conflict of interest.

AUTHOR CONTRIBUTIONS

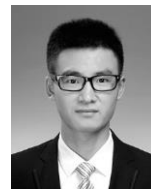
Conceptualization, methodology, software, formal analysis, Ligu Zhou; writing—original draft preparation, Yanshuang Han; review and editing, Hang Wu; Visualization, Hui Li; supervision, Tianliang Zhang.

REFERENCES

- [1] H. Liu, B. Ren, S. Hu, X. Guan, P. Wen, and J. Tang, "High-order dual-band superconducting bandpass filter with controllable bandwidths and multitransmission zeros," *IEEE Trans. Microw. Theory Tech.*, vol. 65, no. 10, pp. 3813–3823, Oct. 2017.
- [2] R. Levy, L. Fellow, and P. Petre, "Design of CT and CQ filters using approximation and optimization," *IEEE Trans. Microw. Theory Tech.*, vol. 49, no. 12, pp. 2350–2356, Dec. 2001.
- [3] J. B. Thomas, "Cross-coupling in coaxial cavity filters — A tutorial overview," *IEEE Trans. Microw. Theory Tech.*, vol. 51, no. 2, pp. 1368–1376, Apr. 2003.
- [4] Y. He, S. Member, G. Wang, X. Song, and L. Sun, "A coupling matrix and admittance function synthesis for mixed topology filters," *IEEE Trans. Microw. Theory Tech.*, vol. 64, no. 2, pp. 4444–4454, Dec. 2016.
- [5] G. Macchiarella, S. Member, M. Oldoni, and S. Tamiazzo, "Narrowband microwave filters with mixed topology," *IEEE Trans. Microw. Theory Tech.*, vol. 60, no. 2, pp. 3980–3987, Dec. 2012.
- [6] S. Li *et al.*, "A 12-pole narrowband highly selective high-temperature superconducting filter for the application in the third-generation wireless communications," *IEEE Trans. Microw. Theory Tech.*, vol. 55, no. 4, pp. 754–759, Apr. 2007.
- [7] J. C. Lu, C. K. Liao, and C. Y. Chang, "Microstrip parallel-coupled filters with cascade trisection and quadruplet responses," *IEEE Trans. Microw. Theory Tech.*, vol. 56, no. 9, pp. 2101–2110, Sep. 2008.
- [8] S. Amari and G. Macchiarella, "Synthesis of inline filters with arbitrarily placed attenuation poles by using nonresonating nodes," *IEEE Trans. Microw. Theory Tech.*, vol. 53, no. 10, pp. 3075–3081, Oct. 2005.
- [9] L. Szydlowski, S. Member, N. Leszczynska, and A. Lamecki, "A substrate integrated waveguide (SIW) bandpass filter in a box con fi

- guration with frequency-dependent coupling," *IEEE Microw. Wireless Compon. Lett.*, vol. 22, no. 11, pp. 556–558, Nov. 2012.
- [10] J. Hong and M. J. Lancaster, "Design of highly selective microstrip bandpass filters with a single pair of attenuation poles at," *IEEE Trans. Microw. Theory Tech.*, vol. 48, no. 7, pp. 1098–1107, Jul. 2000.
- [11] W. Constant, D. Couplings, L. Szydlowski, N. Leszczynska, and M. Mrozowski, "Dimensional synthesis of coupled-resonator pseudoelliptic microwave bandpass filters," *IEEE Trans. Microw. Theory Tech.*, vol. 62, no. 8, pp. 1634–1646, Apr. 2014.
- [12] T. Zhang, K. Yang, H. Zhu, L. Zhou, M. Jiang, and W. Dang, "Miniaturized HTS linear phase filter based on neighboring CQ units sharing resonators," *Supercond. Sci. Technol.*, vol. 28, no. 10, Sep. 2015.
- [13] T. Zhang, K. Yang *et al.*, "Miniature linear-phase superconducting filter with group delay equalization," *Chinese Sci. Bull.*, vol. 55, no. 15, pp. 1453–1458, Apr. 2010.
- [14] T. Zhang, K. Yang, S. Bu, J. Liu, J. Ning, and Z. Luo, "The design of open-loop resonator HTSC linear-phase filter," *Cryogenics*, vol. 47, pp. 409–412, Apr. 2007.
- [15] Q. Chu and H. Wang, "A compact open-loop filter with mixed electric and magnetic coupling," *IEEE Trans. Microw. Theory Tech.*, vol. 56, no. 2, pp. 431–439, Feb. 2008.
- [16] H. Wang, S. Member, and Q. Chu, "An EM-coupled triangular open-loop filter with transmission zeros very close to passband," *IEEE Microw. Wireless Compon. Lett.*, vol. 19, no. 2, pp. 71–73, Feb. 2009.
- [17] H. Wang, S. Member, and Q. Chu, "An inline coaxial quasi-elliptic filter with controllable mixed electric and magnetic coupling," *IEEE Trans. Microw. Theory Tech.*, vol. 57, no. 3, pp. 667–673, Mar. 2009.

Copyright © 2020 by the authors. This is an open access article distributed under the Creative Commons Attribution License which permits unrestricted use, distribution, and reproduction in any medium, provided the original work is properly cited ([CC BY 4.0](https://creativecommons.org/licenses/by/4.0/)).



Ligu Zhou was born in July 1987. He received the M.S. degree in navigation, guidance and control from University of Electronic Science and Technology of China (UESTC), Chengdu, China, in 2016, and is currently pursuing a Ph.D. degree in navigation, guidance and control from UESTC. His research interests include application technology of high temperature superconductor and radio frequency, microwave & millimeter-wave circuits and systems.



Yanshuang Han was born in November 1995. She received the B.Eng. degree in electronic information engineering from Dalian Maritime University (DMU), Dalian, China, in 2019, and is studying for a doctor's degree in control science and engineering from University of Electronic Science and Technology of China (UESTC), Chengdu, China. Her research interests include high temperature superconducting (HTS) microwave & millimeter-wave circuits and systems, RFIC millimeter-wave phased arrays.



Hang Wu was born in November 1990. He received the B.S. degree, in 2012, and the M.S. degree, in 2015, in electronic communication engineering from University of Electronic Science and Technology of China (UESTC), Chengdu, China. His research interests include the spacecraft simulation and fault diagnosis, space launching technology, intelligent mechanical electrical system, and power electronics.

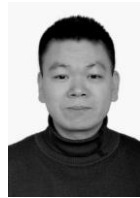


Zhihe Long received his B.E. degree in communication engineering from Nanjing University of Science and Technology (NJUST) in 2015 and M.E. degree in navigation, guidance and control from University of Electronic Science and Technology of China (UESTC) in 2018. He is currently a Ph.D. student at the Dept. of mechanical engineering of City University of Hong Kong. His research interests include high temperature superconducting (HTS) microwave circuits and energy harvesting circuits.



Hui Li received the M.S. degree and the Ph.D. degree from Northwestern Polytechnical University, in 1987 and 1991. He is now working as a professor in University of Electronic Science and Technology of China.

He is currently a professor and the associate dean of the School of Aeronautics and Astronautics, University of Electronic Science & Technology of China, Chengdu, China. He is also a System Simulation Member of the Chinese Society of Automation and a member of China Aerospace and Association. His research interests include the spacecraft simulation and fault diagnosis, space launching technology, intelligent mechanical electrical system, and power electronics.



Tianliang Zhang was born in August 1976. He received the M.S. and Ph.D. degrees in physical electronics from the University of Electronic Science and Technology of China (UESTC), Chengdu, China, in 2004 and 2009, respectively.

He is currently a full-time professor, with UESTC. His research interests include high-temperature superconducting microwave circuits and systems, CAD, CAA, and production technology of high-temperature superconducting microwave circuits.